Applied Clay Science 62–63 (2012) 8–14

Contents lists available at SciVerse ScienceDirect

Applied Clay Science

journal homepage: www.elsevier.com/locate/clay

Effect of reaction temperature on grafting of γ-aminopropyl triethoxysilane (APTES) onto kaolinite

Shu-qin Yang [a,b], Peng Yuan [a,*], Hong-ping He [a], Zong-hua Qin [a,b], Qing Zhou [a,b], Jian-xi Zhu [a], Dong Liu [a]

[a] CAS Key Laboratory of Mineralogy and Metallogeny, Guangzhou Institute of Geochemistry, Chinese Academy of Sciences, Guangzhou 510640, China
[b] Graduate School of Chinese Academy of Sciences, Beijing 100049, China

ARTICLE INFO

Article history:
Received 22 November 2011
Received in revised form 28 March 2012
Accepted 7 April 2012
Available online 17 May 2012

Keywords:
Kaolinite
γ-Aminopropyl triethoxysilane
Grafting

ABSTRACT

The effect of the temperature (175, 185, 195 and 220 °C) on the grafting of γ-aminopropyl triethoxysilane (APTES) on the interlayer hydroxyl groups of kaolinite pre-intercalated with DMSO were investigated using Fourier transform infrared spectroscopy, X-ray diffraction, thermal analysis and elemental analysis. The APTES-modified kaolinite prepared at 220 °C showed a structure with high content of APTES and high thermal stability, in which the APTES molecules were grafted on to the inner-surface hydroxyl groups of kaolinite and arranged in the form of cross-linked monolayers. The APTES-modified kaolinites prepared at 175, 185 and 195 °C exhibited inhomogeneous interlayer structure with pseudo-bilayer arrangements composed of grafted APTES molecules and hydrogen-bound DMSO or APTES molecules coexisting with monolayer arrangements. The monolayer arrangement of APTES corresponded to the basal spacing of about 1.00 nm and the pseudo-bilayer arrangement 1.73–1.89 nm. High reaction temperature was advantageous to the formation of the monolayer arrangement by promoting the exchange of the DMSO molecules by APTES molecules in the interlayer space of kaolinite, as well as the transformation of hydrogen-bound APTES molecules into grafted molecules.

1. Introduction

Over the past decades, organoclay has attracted numerous attentions in clay science (Gelfer et al., 2004; Hanley et al., 2003; Hedley et al., 2007; Lagaly et al., 2006; Xi et al., 2007a), environmental engineering (Beall, 2003; Churchman et al., 2006; Groisman et al., 2004; Nir et al., 2006; Stathi et al., 2007; Sun and Jaffé, 1996) and materials science (Dennis et al., 2001; Liu et al., 2005; Ruiz-Hitzky and Van Meerbeek, 2006). Various methods were proposed to prepare organoclays and the related organoclay-based materials: ion exchange (Lagaly and Beneke, 1991; Xi et al., 2007b), intercalation (Komori et al., 1999; Lagaly, 1986;) and grafting reactions (He et al., 2005; Heinrich et al., 2002; Meerbeek and Ruiz-Hitzky, 1979; Park et al., 2004; Ruiz-Hitzky and Rojo, 1980; Ruiz-Hitzky et al., 1985; Tonlé et al., 2008; Tunney and Detellier, 1993). Organoclay prepared by grafting show excellent chemical, structural and thermal stability because of the covalent bonds between grafted molecules and the clay mineral matrix, enabling promising applications such as environmental remediation (Letaief et al., 2008; Mercier and Detellier, 1995) or nanocomposites (Isoda et al., 2000; Moet and Akelah, 1993).

The most widely used clay minerals in the preparation of surface-grafted organoclays are the 2:1 clay minerals, such as montmorillonite (Mercier and Detellier, 1995; Park et al., 2004; Shanmugharaj et al., 2006; Song and Sandi, 2001), Laponite (Herrera et al., 2005; Park et al., 2004; Wheeler et al., 2005) and hectorite (Guerra et al., 2010). In contrast, kaolinite received less attention for grafting reactions. The interlayer aluminol groups of kaolinite are available for the grafting reactions, the external specific surface area of kaolinite is very small as compared to the interlayer surface area, and the contribution of the hydroxyl groups at the edges or surface defects for the grafting reactions is modest.

For an interlayer grafting of kaolinite, the hydrogen-bound interactions between the structural unites have to be overcome. For this reason, compounds with high dipole moments such as dimethyl sulfoxide (DMSO) should be firstly intercalated into kaolinite before the subsequent grafting. Some researchers had conducted studies on the interlayer grafting of kaolinite (Brandt et al., 2003; Letaief et al., 2008; Tonlé et al., 2007, 2011; Tunney and Detellier, 1993, 1996) with ethylene glycol, ethylene glycol methyl ether, 1, 2-propanediol and 1, 3-propanediol. Some other researchers had also reported the grafted reactions between the inner-surface hydroxyl groups of kaolinite and the small alcohol molecules, such as methanol, ethanolamine, D-sorbitol, adonitol, butanediols, hexanol etc. (Gardolinski and Lagaly, 2005a, 2005b; Itagaki and Kuroda, 2003; Murakami et al., 2004).

In recent years, some efforts in using organosilane for the interlayer grafting of kaolinite were made because the functional groups of organosilane can provide versatile properties such as organophilicity

* Corresponding author. Tel./fax: +86 20 85290341.
E-mail address: yuanpeng@gig.ac.cn (P. Yuan).

0169-1317/$ – see front matter © 2012 Elsevier B.V. All rights reserved.
doi:10.1016/j.clay.2012.04.006

(Gârea et al., 2008), metal affinity (Tan et al., 2011) and enzyme immobilization (Hernando et al., 2007; Kim et al., 2006; Kobayashi and Matsunaga, 1991). Avila et al. (2010) prepared the γ-mercaptopropyl trimethoxysilane-grafted kaolinite and Tonlé et al. (2007) used the γ-aminopropyl triethoxysilane (APTES) grafted kaolinite as coating of platinum electrodes for the use as electrochemical sensor. As the size of most organosilane molecules is much larger than that of the short chain alcohols, rigorous reaction conditions have to be applied to achieve interlayer grafting. These conditions included nitrogen atmosphere, high reaction temperatures, and pure organosilane as the solvent (Kobayashi and Matsunaga, 1991; Tonlé et al., 2007, 2011). Yuan et al. (2008) reported that under mild reaction conditions APTES could not enter the interlayer space of kaolinite or tubular halloysite.

The influence of the reaction temperature during the grafting reactions needs to be clarified because of the previous studies (Avila et al., 2010; Tonlé et al., 2007). Tonlé et al. (2007) prepared the APTES-grafted kaolinite below 195 °C, a temperature slightly below the boiling point of APTES. The grafted derivative displayed the 001 reflection at 1.64 nm, which was proposed as the result of either the APTES species arranged in a nonflattened-configuration or the formation of a bilayer APTES. Avila et al. (2010) reported the APTES-grafted kaolinite prepared below200 °C. The products showed two reflections with *d* values of 18.4 and 9.96 Å and were assigned to the first-order and second-order basal reflections or to two different arrangements of the interlayer silane molecules. In the present study, kaolinite was reacted with APTES at 175, 185, 195 and 220 °C The temperatures of 175 and 185 °C are below the boiling point of the DMSO (189 °C). The upper limit of the temperature was selected as 220 °C because at this temperature the reaction mixture is boiling but pyrolysis of APTES will not occur.

2. Materials and methods

2.1. Materials

The raw kaolinite (Kt) was obtained from Maoming, Guangdong Province, China, and used as received without further purification. Its chemical composition (mass %) was: SiO_2, 46.75; Al_2O_3, 39.15; Fe_2O_3, 1.02; CaO, 0.21; MgO, 0.10; K_2O, 0.25; Na_2O, 0.26; MnO, 0.01; TiO_2, 0.32; P_2O_5, 0.04; ignition loss, 11.92. γ-aminopropyl triethoxysilane (98%) was purchased from Sigma-Aldrich. Dimethyl sulfoxide (DMSO), isopropanol, and 1, 4-dioxane were of analytical grade purity (above 99.7%, Sinopharm Chemical Reagent Co., Ltd) and used as received.

2.2. Preparation of the DMSO-intercalated kaolinite

About 10.0 g kaolinite was dispersed in a mixture of 60.0 mL DMSO and 10.0 mL distilled water. The dispersion was stirred and refluxed at 150 °C for 12 h, followed by aging at room temperature (about 25 °C) for 12 h. The solid material was separated by centrifugation and washed for 3 times with 1, 4-dioxane and isopropanol (2 times) to eliminate the excess DMSO. The product was air-dried at 60 °C for 24 h, and ground to powder. The final DMSO-intercalated kaolinite is denoted as Kt-D.

2.3. Grafting reaction

A dispersion of Kt-D (2.0 g) in 10.0 mL of APTES under N_2 atmosphere was refluxed at 48 h at 175, 185, 195 and 220 °C. The products were centrifuged and washed 6 times with isopropanol and dried at 80 °C for 12 h (Kt-D-A/175, Kt-D-A/185, Kt-D-A/195, and Kt-D-A/220).

2.4. Hydrolysis and condensation of APTES

The hydrolyzed product of APTES at ambient condition was used as a reference sample. It was prepared according to the following procedures: 3.0 mL APTES solution was dried at ambient condition (the room temperature was about 25 °C and the relative humidity was about 77%) for 12 h. The dried product (denoted as Hydro-A) was a white solid which was also ground to powder. Hydro-A samples were heated at 200, 300, 400, and 600 °C for 4 h under N_2 atmosphere (Hydro-A/200, Hydro-A/300, Hydro-A/400, and Hydro-A/600).

3. Characterization

The CHNS elemental analyses were performed on an Elementar Vario EL III Universal CHNOS elemental analyzer. The content of loaded APTES (M_{APTES}, mmol silane/g sample) was determined by $M_{APTES} = W_N / M_N$, where W_N was the content (mass %) of nitrogen obtained by the elemental analysis. M_N was the molar mass of N (14.01 g/mol). The content of DMSO in the modified kaolinite was derived from the sulfur content.

Infrared spectra were acquired on a Bruker Vertex-70 Fourier transform infrared spectrometer using 64 scans with a resolution of 2 cm^{-1}. The specimens for the measurements were prepared by mixing the sample powder with KBr at an appropriate ratio and pressing the mixtures into transparent pellets.

X-ray diffraction patterns were obtained on a Bruker D8 advanced diffractometer (Cu Kα radiation, λ = 0.154 nm, 40 kV, 40 mA). The scan rate was 1° (2θ)/min.

Thermal analyses were performed on a Netzsch STA 409 PC instrument under nitrogen flow (60 mL/min) at a heating rate of 5 °C/min. Approximately 20 mg of sample was used in each run.

4. Results and discussion

4.1. Elemental and FTIR analysis

The contents of the introduced APTES and the residual DMSO in the modified kaolinites are shown in Fig. 1. The amount of APTES increased with the reaction temperatures and Kt-D-A/220 exhibited the largest loading (0.67 mmol/g). In contrast with that, the content of DMSO in the APTES-modified samples gradually decreased with increasing reaction temperature. Kt-D-A/220 contained only a small amount of DMSO (0.20 mmol/g) (Fig. 1). Thus, the intercalation of APTES in kaolinite proceeded by displacement of DMSO, and a high reaction temperature was advantageous for promoting both processes.

The FTIR spectra of kaolinite, DMSO-intercalated kaolinite and the APTES-modified kaolinite samples are presented in Fig. 2a. The frequency and assignments of the main vibrations are listed in Table 1.

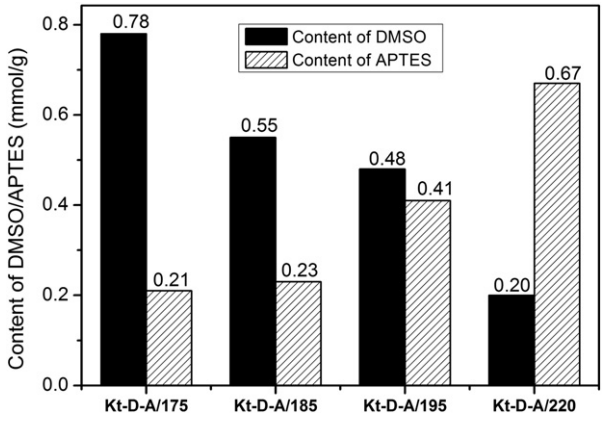

Fig. 1. The content of DMSO and APTES in the modified kaolinites.

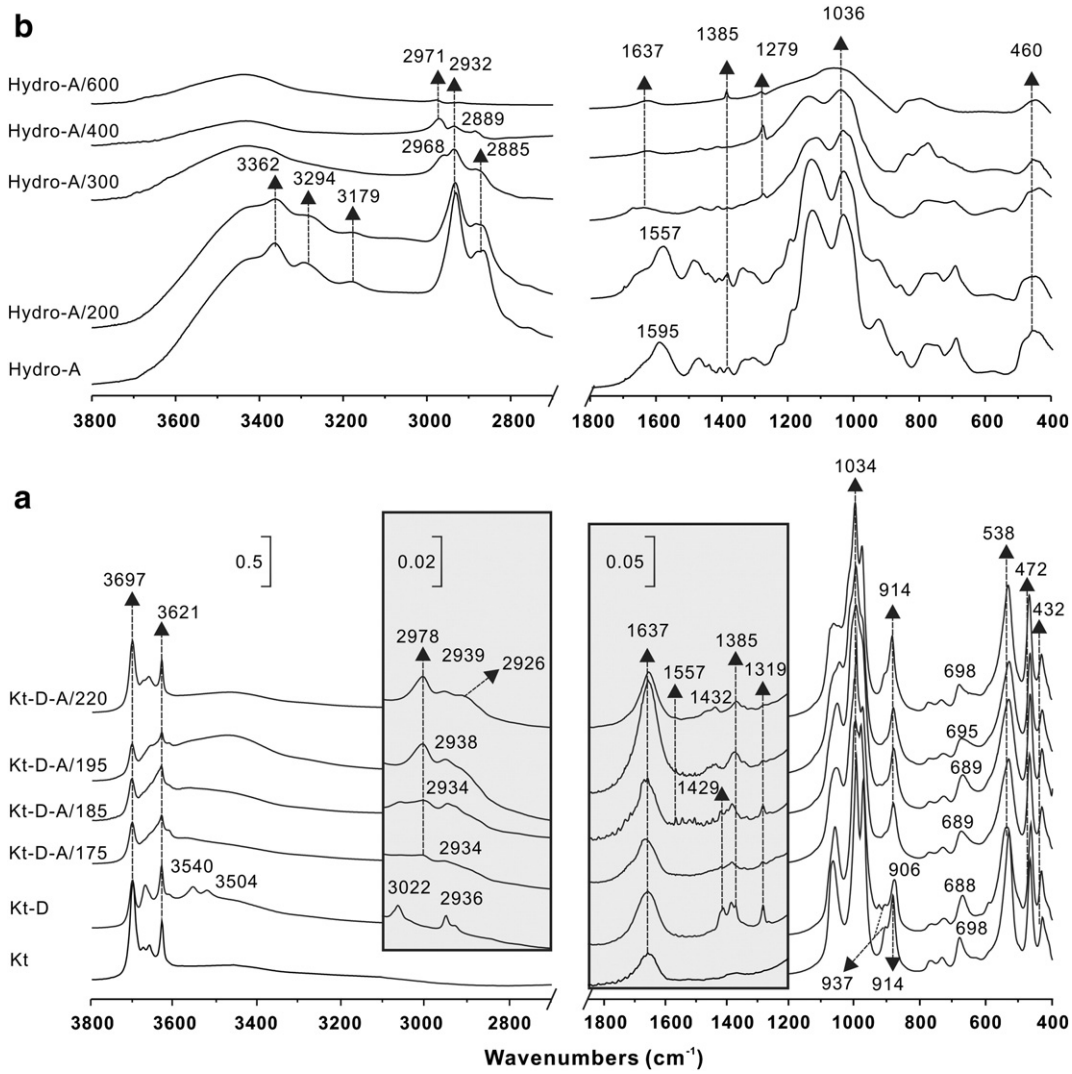

Fig. 2. FTIR spectra of (a) kaolinite, DMSO intercalated kaolinite and the APTES-modified kaolinites; and (b) Hydro-A and its heat-treated samples.

Table 1
Positions and assignments of the IR vibration bands of the APTES-modified kaolinites (Avila et al., 2010; Tonlé et al., 2007; Yuan et al., 2008).

Position (cm^{-1})	Assignments	Position (cm^{-1})	Assignments
3697, 3654	Inner-surface Al–OH stretching	1107	Si–O symmetric stretching
3621	Inner Al–OH stretching	1033, 1009	Si–O asymmetric stretching
2978	C–H_3 asymmetric stretching	914, 912	Inner Al–OH deformation
2939, 2936, 2934	C–H_2 asymmetric stretching	797	Si–O symmetric stretching
2906	C–H_3 symmetric stretching	755	Si–O stretching, Si–O–Al translation
1634	O–H deformation of absorbed water	695, 689, 688	Si–O stretching
1557	N–H_2 deformation (scissoring)	645	Al–O stretching, Si–O–Al translation
1432, 1429	CH_2 deformation	538	Si–O–Al deformation
1385	CH_2 deformation (wagging)	472	Si–O–Si deformation
1319	C–H_2 twisting vibration	432	Si–O deformation

These assignments were based on previous reports on kaolinite and APTES-modified materials (Avila et al., 2010; Tonlé et al., 2007; Yuan et al., 2008). Kt displayed the typical stretching vibrations of the inner-surface hydroxyl groups at 3697, 3669 and 3653 cm^{-1}, and that of the inner hydroxyl groups at 3621 cm^{-1}. Two new bands in the spectrum of Kt-D (3504 and 3540 cm^{-1}) should result from the bonding of the DSMO molecules with the inner-surface hydroxyl groups of the kaolinite layers (Frost et al., 1998). The stretching vibrations related to the hydroxyl groups were obviously affected by the guest molecules (Fig. 2a). New bands of asymmetric C–H_3 stretching (3022 cm^{-1}), symmetric C–H_3 stretching (2936 cm^{-1}), asymmetric C–H_3 deformation (1445–1414 cm^{-1}) and symmetric C–H_3 deformation (1319 cm^{-1}) reflected the existence of the DMSO molecules in Kt-D (Johnston et al., 1984).

The APTES-modified kaolinite samples exhibited some new vibration bands (Fig. 2a), including the asymmetric stretching vibrations of C–H_3 and C–H_2 at 2978 and 2938 cm^{-1}, the N–H_2 deformation vibration at 1557 cm^{-1}, the deformation C–H_2 vibration at 1429 cm^{-1}, the deformation (wagging) vibration of C–H_2 at 1385 cm^{-1}, and the twisting vibration of C–H_2 at 1319 cm^{-1}. The spectra of all APTES-modified kaolinites showed decreasing intensities of the OH stretching vibrations

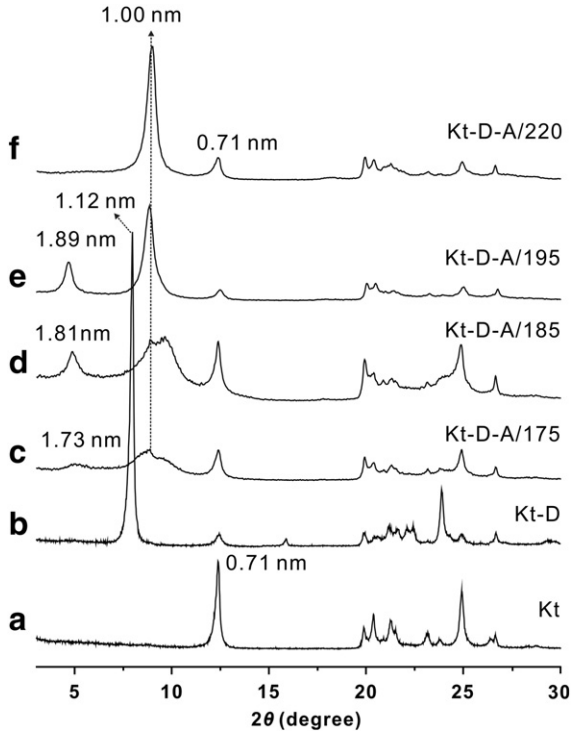

Fig. 3. X-ray powder diffraction patterns of kaolinite, DMSO intercalated kaolinite and the APTES-modified kaolinites.

(3697 and 3669 cm^{-1}) of the inner-surface Al–OH groups as compared to the spectrum of Kt, suggesting that the modification was accompanied by the consumption of inner-surface Al–OH groups. These results indicated that grafting has taken place between the inner-surface Al–OH groups and the hydrolyzed APTES.

Grafting transformed the Si–O–Si stretching vibrations (1107, 1033 and 1009 cm^{-1}) gradually into one broad vibration band (Fig. 2a), indicating that the Si–O skeletal bands were dramatically perturbed by the introduced APTES. These changes gave some additional support for the grafting of APTES.

Fig. 2b presented the FTIR spectra of heated Hydro-A. The N–H_2 stretching vibrations of Hydro-A were observed at 3362, 3294 and 3179 cm^{-1}, and the bending vibration was at 1595 cm^{-1}. Hydro-A/200 showed a spectrum similar to that of Hydro-A. In the case of Hydro-A/300, the N–H_2 vibration bands disappeared, indicating the removal of the amino groups by combustion. Thus, intensities of the C–H vibrations decreased. In the spectrum of Hydro-A/400 the C–H vibration bands were very weak, and for Hydro-A/600 were almost absent. This indicated that the thermal decomposition of the C–H groups occurred at 300–600 °C.

4.2. XRD results

Kt showed the typical XRD pattern of kaolinite with the characteristic basal spacing of 0.71 nm (Fig. 3a). Kt-D showed an enlarged basal spacing of 1.12 nm (Fig. 3b), due to the intercalation of the DMSO (Olejnik et al., 1970). The intercalation degree (I.R.) was 95%, calculated from: I.R. $= I_I/(I_K + I_I)$, where I_K is the intensity of the 001 reflection of the unreacted kaolinite, I_I is the 001 reflection of the DMSO intercalated kaolinite (Lagaly et al., 2006).

Several new reflections were observed in the XRD patterns of the APTES-modified kaolinites. Kt-D-A/175 (Fig. 3c) showed two weak reflections with d value of 1.73 and about 1.00 nm, respectively. These reflections were intensified in the XRD pattern of Kt-D-A/185 (Fig. 3d) and became intense and symmetric in that of Kt-D-A/195 (Fig. 3e). However, only the reflection with d = 1.00 nm remained in the XRD pattern of Kt-D-A/220 (Fig. 3f).

In the previous reports, Tonlé et al. (2007) and Avila et al. (2010) prepared the APTES-modified kaolinites at 195 and 200 °C, APTES did not decompose at these temperatures. That means the 1.00 nm basal spacing did not result from the small grafted units formed by the decomposition of APTES but should from the arrangement of flatly lying APTES molecules in monolayer in the interlayer space of kaolinite (Fig. 4d). This assignment was well supported by the lateral size of the hydrolyzed APTES, whose lateral cross-section was about 0.33 nm according to a stereochemical calculation.

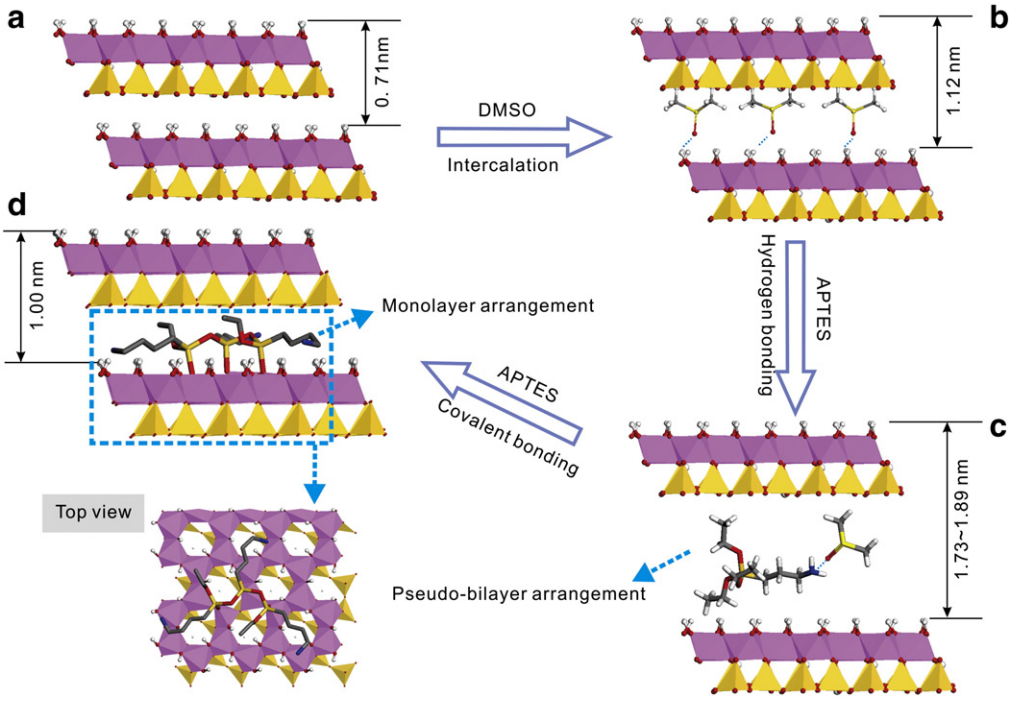

Fig. 4. Schematic descriptions of the proposed bonding modes.

The 1.73–1.89 nm spacing should result from some forms of bilayer arrangements, which may consist of APTES and DMSO molecules. The amino-head of APTES can be readily hydrogen-bound with the interlayer hydroxyl groups and the oxygen atoms of DMSO were also easily hydrogen-bound with APTES, it is likely that the 1.73 nm *d* value of Kt-D-A/175 resulted from a pseudo-bilayer arrangement of APTES molecules combined with hydrogen-bound DMSO. However, in the cases of Kt-D-A/185 and Kt-D-A/195, the higher reaction temperatures promoted the removal of DMSO so that more APTES molecules replaced DMSO yielding the larger basal spacing of 1.81 and 1.89 nm. The above-mentioned monolayer and pseudo-bilayer structures should coexist in Kt-D-A/175 and Kt-D-A/185 (Fig. 4c). The 001 reflection in both cases was broadened indicating low crystallinity and stacking order, which further supports the inhomogeneous intercalation. It is noteworthy that a small amount APTES might be also bound on the inner surface of kaolinite by electrostatic interaction because the basic character of the amine might cause proton transfer from the acidic hydroxyl groups, resulting in an electrostatic interaction between $-NH_3^+$ and surface O^- (Vrancken et al., 1995). However, the electrostatic interaction of perhaps a very few molecules evidently did not change the interlayer distance of the kaolinite.

The monolayer arrangement of flatly lying APTES molecules corresponding to a basal spacing of about 1.00 nm was well developed in Kt-D-A/195. The reason might be that many hydrogen-bonds between APTES and the interlayer aluminol groups were formed and APTES molecules condensed with the neighboring aluminol groups (Vrancken et al., 1995). Note that the amine groups did not take part in the grafting process, and the alkyl groups were pointed away from the surface. Thus, the aminosilane molecules were turned over from their initial amine-down position in hydrogen-bond state to a final amine-up position. A similar mechanism of the formation of covalent-bonds was verified by Linde (1990) and Vrancken et al. (1995) in the system of aminosilane and SiO_2 under an anhydrous condition. This process was promoted at 220 °C, and most of the previously hydrogen-bound APTES molecules were involved in the condensation with the interlayer aluminol groups of kaolinite and transformed into the grafted state, because Kt-D-A/220 showed a homogeneous monolayer structure as indicated by the dominant d-value of 1.00 nm.

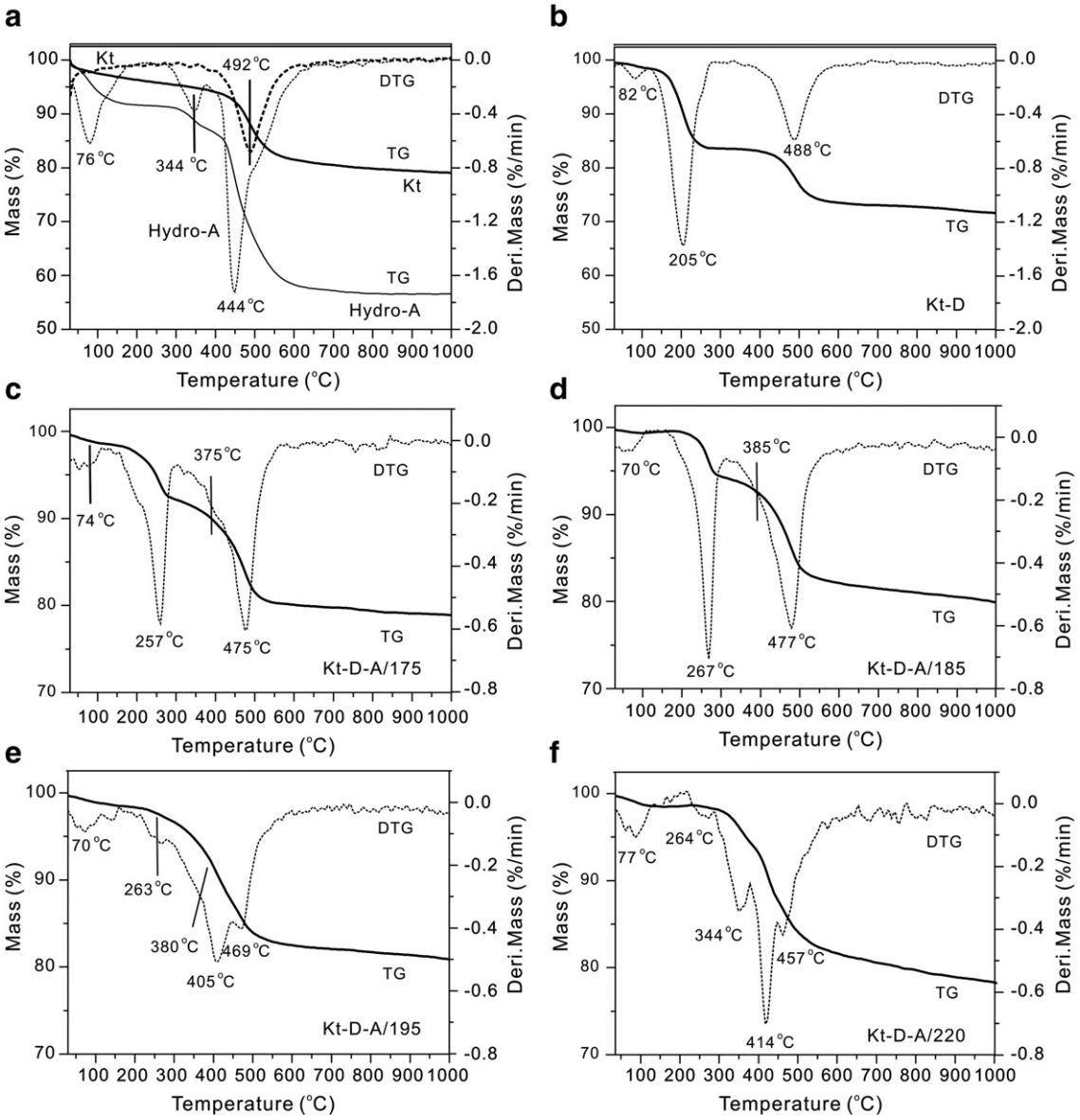

Fig. 5. TG and DTG curves (30-1000 °C) of (a) kaolinite and Hydro-A; (b) DMSO intercalated kaolinite; and (c, d, e, f) the APTES-modified kaolinites.

4.3. TG analysis

The TG curve of Kt showed one major mass loss corresponding to the DTG peak centered at 492 °C (Fig. 5a) and attributed to the dehydroxylation of kaolinite. Kt-D (Fig. 5b) exhibited two major mass losses, centering at 488 and 205 °C. The former one resulted from the dehydroxylation of kaolinite and the latter from the elimination of DMSO (Frost et al., 1999). There was also a very minor mass loss at about 82 °C. It is attributed to absorbed water introduced during the DMSO intercalation.

Three mass losses were resolved in the TG/DTG curves of Hydro-A. The first one in range of 30–180 °C with the DTG peak centered at 76 °C was attributed to the removal of absorbed water and APTES molecules (Fig. 5a). The second one at 250–380 °C with the DTG peak centered at 344 °C was assigned to the removal of nitrogenous fragments during combustion. The mass loss between 430 °C and about 600 °C may be attributed to the decomposition of the oxyethyl groups. These assignments are in good agreement with the previous study on the hydrolysis of APTES (Tonlé et al., 2007) and also supported by the FTIR results of the heated Hydro-A as discussed above. As shown in Fig. 2b, all the $N-H_2$ vibration bands were weakened in the spectrum Hydro-A/200 and disappeared in that of Hydro-A/300. However, the decomposition of the C–H groups was complete only at 600 °C.

Kt-D-A/175 exhibited a large mass loss at about 257 °C (Fig. 5c). It is attributed to the volatilization of the intercalated organic compounds, which were mostly hydrogen-bound so that they were volatilized at a much lower temperature than the grafted APTES. They mainly consisted of residual DMSO molecules, as well as small amounts of hydrogen-bound APTES. This assumption is supported by the analytical data. The content of DMSO in Kt-D-A/175, calculated by elemental analysis, was 6.09%, but Kt-D-A/175 exhibited a mass loss of 6.29% at 160–280 °C.

In the DTG curve of Kt-D-A/185 (Fig. 5d), the center of this mass loss peak slightly shifted to about 267 °C and became more symmetric, suggesting a higher content of hydrogen-bound APTES and less DMSO. Accordingly, the DMSO content in Kt-D-A/185 was 4.29% but the mass loss at 160–280 °C was 5.38%.

The mass loss corresponding to the dehydroxylation of kaolinite in Kt-D-A/175, centered at about 475 °C, was smaller than that of Kt. This implied that some inner-surface aluminol groups had been grafted with APTES. The shoulder DTG peak at about 380 °C should be attributed to the decomposition of the grafted APTES.

The major DTG peak at about 405 °C was showed in the case of Kt-D-A/195 (Fig. 5e) is due to the decomposition of the grafted APTES arranged in monolayer. The mass loss at about 263 °C was smaller than for Kt-D-A/185. However, the monolayers structure was well developed in Kt-D-A/195 as evidenced by the basal spacing of 1.00 nm (Fig. 2e). This fact suggested that the bilayer structure with the basal spacing of 1.89 nm was mainly composed of grafted APTES and the hydrogen-bound APTES whereas DMSO was almost completely displaced.. The mass losses centered at 344 and 414 °C in the DTG curve of Kt-D-A/220 were caused by the decomposition of the nitrogen-containing fragments and the pyrolysis of the oxyethyl groups of the grafted APTES, because the monolayer structure of APTES was dominant and DMSO was displaced. The small mass loss at 264 °C indicated that the amount of hydrogen-bound APTES was very small. A more quantitative interpretation of the TG data t was difficult because the decomposition stages of different APTES/DMSO species and the dehydroxylation of kaolinite partially overlapped.

The above discussion indicated two major effects of the reaction temperatures on APTES structure: (i) increasing reaction temperature promoted the displacement of DMSO by APTES; (ii) the high reaction temperature promoted the condensation on the silicon side of the APTES and the subsequent formation of covalent bonds between APTES and the inner surface of kaolinite. As a result, the interlamellar pseudo-bilayer arrangement of APTES molecules was rearranged into the monolayer arrangement.

In conclusion, the reaction temperature not only promoted the grafting reaction but also the APTES arrangement. Several potential applications can be postulated. For example, the monolayer of grafted APTES monolayer molecules may be used as a precursor for further introduction of some functional guest molecules through hydrogen bonding or electrostatic attraction, or for some adsorption purposes. Moreover, organosilane modified kaolinites with adjustable properties could be designed by simply changing the functional head-groups of the silanes, enabling versatile uses of the organosilane/kaolinite hybrids.

5. Conclusions

The reaction temperature had significant effects on the grafting of APTES in the interlayer space of kaolinite. High temperature (220 °C) accelerated the diffusion of APTES into the interlayer region and desorption of DMSO out of the interlayer space. It also promoted the condensation of the APTES groups on the silicon side with the inner-surface hydroxyl groups of kaolinite and the subsequent interlamellar grafting of APTES. A monolayer structure composed of grafted APTES formed in the interlayer space below 220 °C. At lower temperatures, a pseudo-bilayer structure composed of the grafted APTES molecules and hydrogen-bound DMSO or APTES molecules, together the monolayer structure was formed. These results demonstrated that different interlayer structures can be obtained by simply adjusting the reaction temperatures, enabling promising applications of the kaolinite/APTES hybrid materials.

Acknowledgment

This work was financially supported by the National Natural Science Foundation of China (Grant No. U0933003), the Knowledge Innovation Program of the Chinese Academy of Sciences (Grant No. KZCX2-YW-QN101) and the National Science Fund for Distinguished Young Scholars (Grant No. 40725006). This is a contribution (No. IS1466) from GIGCAS.

References

Avila, L.R., de Faria, E.H., Ciuffi, K.J., Nassar, E.J., Calefi, P.S., Vicente, M.A., Trujillano, R., 2010. New synthesis strategies for effective functionalization of kaolinite and saponite with silylating agents. Journal of Colloid and Interface Science 341 (1), 186–193.

Beall, G.W., 2003. The use of organo-clays in water treatment. Applied Clay Science 24 (1–2), 11–20.

Brandt, K.B., Elbokl, T.A., Detellier, C., 2003. Intercalation and interlamellar grafting of polyols in layered aluminosilicates. D-sorbitol and adonitol derivatives of kaolinite. Journal of Materials Chemistry 13 (10), 2566–2572.

Churchman, G.J., Gates, W.P., Theng, B.K.G., Yuan, G., 2006. Clays and clay minerals for pollution control. In: Bergaya, F., Theng, B.K.G., Lagaly, G. (Eds.), Handbook of Clay Science. Developments in Clay Science, vol. 1. Elsevier, Amsterdam, pp. 625–675.

Dennis, H.R., Hunter, D.L., Chang, D., Kim, S., White, J.L., Cho, J.W., Paul, D.R., 2001. Effect of melt processing conditions on the extent of exfoliation in organoclay-based nanocomposites. Polymer 42 (23), 9513–9522.

Frost, R.L., Kristof, J., Paroz, G.N., Kloprogge, J.T., 1998. Molecular structure of dimethyl sulfoxide intercalated kaolinites. The Journal of Physical Chemistry. B 102 (43), 8519–8532.

Frost, R., Kristof, J., Horvath, E., Kloprogge, J.T., 1999. Deintercalation of dimethylsulphoxide intercalated kaolinites—a DTA/TGA and Raman spectroscopic study. Thermochimica Acta 327 (1–2), 155–166.

Gardolinski, J.E.F.C., Lagaly, G., 2005a. Grafted organic derivatives of kaolinite: I. Synthesis, chemical and rheological characterization. Clay Minerals 40 (4), 537–546.

Gardolinski, J.E.F.C., Lagaly, G., 2005b. Grafted organic derivatives of kaolinite: II. Intercalation of primary n-alkylamines and delamination. Clay Minerals 40 (4), 547–556.

Gârea, S.A., Iovu, H., Bulearca, A., 2008. New organophilic agents of montmorillonite used as reinforcing agent in epoxy nanocomposites. Polymer Testing 27 (1), 100–113.

Gelfer, M., Burger, C., Fadeev, A., Sics, I., Chu, B., Hsiao, B.S., Heintz, A., Kojo, K., Hsu, S.L., Si, M., Rafailovich, M., 2004. Thermally induced phase transitions and morphological changes in organoclays. Langmuir 20 (9), 3746–3758.

Groisman, L., Rav-Acha, C., Gerstl, Z., Mingelgrin, U., 2004. Sorption of organic compounds of varying hydrophobicities from water and industrial wastewater by long- and short-chain organoclays. Applied Clay Science 24 (3–4), 159–166.
Guerra, D.L., Airoldi, C., Viana, R.R., 2010. Retracted: modification of hectorite by organofunctionalization for use in removing U(VI) from aqueous media: thermodynamic approach. Journal of Environmental Radioactivity 101 (2), 122–133.
Hanley, H.J.M., Muzny, C.D., Ho, D.L., Glinka, C.J., 2003. A small-angle neutron scattering study of a commercial organoclay dispersion. Langmuir 19 (14), 5575–5580.
He, H., Duchet, J., Galy, J., Gerard, J.F., 2005. Grafting of swelling clay materials with 3-aminopropyl triethoxysilane. Journal of Colloid and Interface Science 288 (1), 171–176.
Hedley, C.B., Yuan, G., Theng, B.K.G., 2007. Thermal analysis of montmorillonites modified with quaternary phosphonium and ammonium surfactants. Applied Clay Science 35 (3–4), 180–188.
Heinrich, T.P., Beneke, K., Lagaly, G., 2002. Silylation of a crystalline silicic acid: an MAS NMR and porosity study. Journal of Materials Chemistry 12 (10).
Hernando, J., Pourrostami, T., Garrido, J.A., Williams, O.A., Gruen, D.M., Kromka, A., Steinmüller, D., Stutzmann, M., 2007. Immobilization of horseradish peroxidase via an amino silane on oxidized ultrananocrystalline diamond. Diamond and Related Materials 16 (1), 138–143.
Herrera, N.N., Letoffe, J.M., Reymond, J.P., Bourgeat-Lami, E., 2005. Silylation of laponite clay particles with monofunctional and trifunctional vinyl alkoxysilanes. Journal of Materials Chemistry 15 (8), 863–871.
Isoda, K., Kuroda, K., Ogawa, M., 2000. Interlamellar grafting of γ-methacryloxypropylsilyl groups on magadiite and copolymerization with methyl methacrylate. Chemistry of Materials 12 (6), 1702–1707.
Itagaki, T., Kuroda, K., 2003. Organic modification of the interlayer surface of kaolinite with propanediols by transesterification. Journal of Materials Chemistry 13 (5), 1064–1068.
Johnston, C.T., Sposito, G., Bocian, D.F., Birge, R.R., 1984. Vibrational spectroscopic study of the interlamellar kaolinite–dimethyl sulfoxide complex. Journal of Physical Chemistry 88 (24), 5959–5964.
Kim, J., Grate, J.W., Wang, P., 2006. Nanostructures for enzyme stabilization. Chemical Engineering Science 61 (3), 1017–1026.
Kobayashi, H., Matsunaga, T., 1991. Amino-silane modified superparamagnetic particles with surface-immobilized enzyme. Journal of Colloid and Interface Science 141 (2), 505–511.
Komori, Y., Sugahara, Y., Kuroda, K., 1999. Intercalation of alkylamines and water into kaolinite with methanol kaolinite as an intermediate. Applied Clay Science 15 (1–2), 241–252.
Lagaly, G., 1986. Interaction of alkylamines with different types of layered compounds. Solid State Ionics 22 (1), 43–51.
Lagaly, G., Beneke, K., 1991. Intercalation and exchange reactions of clay minerals and non-clay layer compounds. Colloid & Polymer Science 269 (12), 1198–1211.
Lagaly, G., Ogawa, M., Dékány, I., 2006. Clay mineral organic interactions. In: Bergaya, F., Theng, B.K.G., Lagaly, G. (Eds.), Handbook of Clay Science. Developments in Clay Science, vol. 1. Elsevier, Amsterdam, pp. 309–377.
Letaief, S., Tonle, I.K., Diaco, T., Detellier, C., 2008. Nanohybrid materials from interlayer functionalization of kaolinite: application to the electrochemical preconcentration of cyanide. Applied Clay Science 42 (1–2), 95–101.
Linde, H.G., 1990. Polyamic acid interactions with aminopropyl silane surface conditioners on metal. Journal of Applied Polymer Science 40 (3–4), 613–622.
Liu, W., Hoa, S.V., Pugh, M., 2005. Organoclay-modified high performance epoxy nanocomposites. Composites Science and Technology 65 (2), 307–316.
Meerbeek, A.V., Ruiz-Hitzky, E., 1979. Mechanism of the grafting of organosilanes on mineral surfaces II. Secondary reaction during the grafting of alkenyl chlorosilanes. Colloid and Polymer Science 257 (2), 178–181.
Mercier, L., Detellier, C., 1995. Preparation, characterization, and applications as heavy metals sorbents of covalently grafted thiol functionalities on the interlamellar surface of montmorillonite. Environmental Science and Technology 29 (5), 1318–1323.
Moet, A.S., Akelah, A., 1993. Polymer-clay nanocomposites: polystyrene grafted onto montmorillonite interlayers. Materials Letters 18 (1–2), 97–102.
Murakami, J., Itagaki, T., Kuroda, K., 2004. Synthesis of kaolinite-organic nanohybrids with butanediols. Solid State Ionics 172 (1–4), 279–282.
Nir, S., El-Nahhal, Y., Undabeytia, T., Rytwo, G., Polubesova, T., 2006. Clays and pesticides. In: Bergaya, F., Theng, B.K.G., Lagaly, G. (Eds.), Handbook of Clay Science. Developments in Clay Science, vol. 1. Elsevier, Amsterdam, pp. 677–692.
Olejnik, S., Posner, A.M., Quirk, J.P., 1970. The intercalation of polar organic compounds into kaolinite. Clay Minerals 8, 421–434.
Park, M., Shim, I.K., Jung, E.Y., Choy, J.H., 2004. Modification of external surface of laponite by silane grafting. Journal of Physics and Chemistry of Solids 65 (2–3), 499–501.
Ruiz-Hitzky, E., Rojo, J.M., 1980. Intracrystalline grafting on layer silicic acids. Nature 287 (5777), 28–30.
Ruiz-Hitzky, E., Van Meerbeek, A., 2006. Clay mineral- and organoclay-polymer nanocomposite. In: Bergaya, F., Theng, B.K.G., Lagaly, G. (Eds.), Handbook of Clay Science. : Developments in Clay Science, vol. 1. Elsevier, Amsterdam, pp. 583–621.
Ruiz-Hitzky, E., Rojo, J.M., Lagaly, G., 1985. Mechanism of the grafting of organosilanes on mineral surfaces. Colloid & Polymer Science 263 (12), 1025–1030.
Shanmugharaj, A.M., Rhee, K.Y., Ryu, S.H., 2006. Influence of dispersing medium on grafting of aminopropyl triethoxysilane in swelling clay materials. Journal of Colloid and Interface Science 298 (2), 854–859.
Song, K., Sandi, G., 2001. Characterization of montmorillonite surfaces after modification by organosilane. Clays and Clay Minerals 49 (2), 119–125.
Stathi, P., Litina, K., Gournis, D., Giannopoulos, T.S., Deligiannakis, Y., 2007. Physicochemical study of novel organoclays as heavy metal ion adsorbents for environmental remediation. Journal of Colloid and Interface Science 316 (2), 298–309.
Sun, S., Jaffé, P.R., 1996. Sorption of phenanthrene from water onto alumina coated with dianionic surfactants. Environmental Science and Technology 30 (10), 2906–2913.
Tan, G., Zhang, L., Ning, C., Liu, X., Liao, J., 2011. Preparation and characterization of APTES films on modification titanium by SAMs. Thin Solid Films 519 (15), 4997–5001.
Tonlé, I.K., Diaco, T., Ngameni, E., Detellier, C., 2007. Nanohybrid kaolinite-based materials obtained from the interlayer grafting of 3-aminopropyl triethoxysilane and their potential use as electrochemical sensors. Chemistry of Materials 19 (26), 6629–6636.
Tonlé, I.K., Ngameni, E., Tcheumi, H.L., Tchiéda, V., Carteret, C., Walcarius, A., 2008. Sorption of methylene blue on an organoclay bearing thiol groups and application to electrochemical sensing of the dye. Talanta 74 (4), 489–497.
Tonlé, I.K., Letaief, S., Ngameni, E., Walcarius, A., Detellier, C., 2011. Square wave voltammetric determination of lead(II) ions using a carbon paste electrode modified by a thiol-functionalized kaolinite. Electroanalytical 23 (1), 245–252.
Tunney, J.J., Detellier, C., 1993. Interlamellar covalent grafting of organic units on kaolinite. Chemistry of Materials 5 (6), 747–748.
Tunney, J.J., Detellier, C., 1996. Chemically modified kaolinite: grafting of methoxy groups on the interlamellar aluminol surface of kaolinite. Journal of Materials Chemistry 6 (10), 1679–1685.
Vrancken, K.C., Possemiers, K., Van Der Voort, P., Vansant, E.F., 1995. Surface modification of silica gels with aminoorganosilanes. Colloids and Surfaces A 8 (3), 235–241.
Wheeler, P.A., Wang, J., Baker, J., Mathias, L.J., 2005. Synthesis and characterization of covalently functionalized laponite clay. Chemistry of Materials 17 (11), 3012–3018.
Xi, Y., Frost, R.L., He, H., 2007a. Modification of the surfaces of Wyoming montmorillonite by the cationic surfactants alkyl trimethyl, dialkyl dimethyl, and trialkyl methyl ammonium bromides. Journal of Colloid and Interface Science 305 (1), 150–158.
Xi, Y., Zhou, Q., Frost, R.L., He, H., 2007b. Thermal stability of octadecyltrimethyl ammonium bromide modified montmorillonite organoclay. Journal of Colloid and Interface Science 311 (2), 347–353.
Yuan, P., Southon, P.D., Liu, Z., Green, M.E.R., Hook, J.M., Antill, S.J., Kepert, C.J., 2008. Functionalization of halloysite clay nanotubes by grafting with γ-aminopropyl triethoxysilane. Journal of Physical Chemistry C 112 (40), 15742–15751.